

Extended organization of colloidal microparticles by surface plasmon polariton excitation

V. Garcés-Chávez,¹ R. Quidant,^{2,3} P. J. Reece,¹ G. Badenes,² L. Torner,² and K. Dholakia^{1,*}
¹*SUPA, School of Physics and Astronomy, University of St. Andrews, North Haugh, St. Andrews KY16 9SS, Scotland*
²*ICFO–Institut de Ciències Fotoniques, Jordi Girona 29, Nexus II, 08034 Barcelona, Spain*
³*ICREA–Institució Catalana de Recerca i Estudis Avançats, 08010 Barcelona, Spain*

(Received 22 September 2005; revised manuscript received 19 December 2005; published 21 February 2006)

In this paper we demonstrate the first use of enhanced optical forces and optically induced thermophoretic and convective forces produced by surface plasmon polariton excitation for large-scale ordering and trapping of colloidal aggregations. We identify regimes in which each of these forces dominate the colloidal dynamics and lead to different collective equilibrium states. These include accumulation and organization into hexagonal close-packed colloidal crystals, arrangement into linear colloidal particle chains, and the formation of colloids in a ring formation about the excited region.

DOI: [10.1103/PhysRevB.73.085417](https://doi.org/10.1103/PhysRevB.73.085417)

PACS number(s): 81.16.Dn, 82.60.Lf, 82.70.Dd, 87.80.Cc

I. INTRODUCTION

Metal-dielectric interfaces sustain resonant electromagnetic modes corresponding to a collective oscillation of free electrons with the incident field.¹ Such surface plasmon polaritons (SPP) have a number of unique optical properties, which make them amenable to applications where classical optics is fundamentally restricted.² These applications include apertureless optical nanolithography with resolution comparable to electron beam lithography,³ compact integrated optical and/or electrical nanostructures with subwavelength dimensions (plasmonics),⁴ single molecule detection using surface enhanced Raman scattering (SERS),⁵ and recently super-lensing effects for subdiffraction limited imaging.⁶ In short, surface plasmons offer a powerful tool for extending the role of photonics in existing and potentially new fields.

Conventional optical trapping uses optical gradient forces present in a single highly focused laser beam to confine small numbers of particles at the beam focus.⁷ Optical traps may also be multiplexed using technology such as acousto-optic deflectors or spatial light modulators to create arbitrary trap geometries for small colloidal arrays.⁸ However the requirement of the order of 1 mW per trap site increases the minimum power for large-scale arrays using multiple optical traps. Within this remit, recently the use of evanescent wave (EW) trapping geometries has shown the ability to manipulate large extended two-dimensional (2D) arrays of particles on a dielectric surface using the gradient force.⁹ A colloidal particle placed in the vicinity of an evanescent wave will experience an optical force due to the presence of the large intensity gradient and may be guided preferentially along the surface of the dielectric, in the direction of the transverse component of EW wave vector.¹⁰ Through the use of counter-propagating evanescent fields or by patterning the evanescent field, several hundred colloids may be stably trapped and/or manipulated simultaneously.⁹ Potentially, any enhancement to this optical interaction should yield a system where optical forces can trap particles over a significantly larger surface area: in this respect the use of surface plasmons potentially offer added value as they produce an enhanced evanescent electric field at the surface, which in turn

results in a stronger optical interaction with the trapped colloids. Such enhancement of optical forces has previously been demonstrated in the atomic regime for fabricating SPP based atomic mirrors.¹¹

In addition to the enhanced optical field, the excitation of surface plasmon polaritons also generates local heating, producing thermal gradients within the adjacent medium. Such optically induced thermal effects can be used to locally control forces within the medium and may be an effective tool for manipulating particles on the microscopic scale.^{12,13} For example, surface plasmon induced thermal gradients can manipulate liquid droplets on a surface via Marangoni effects.¹⁴ In general thermal gradients at the microscopic scale are known to induce convection and thermophoresis. Under a thermal gradient, colloids are driven towards the cold region by thermal diffusion (thermophoresis). On the other hand, convection acts to circulate fluid around a volume in order to transfer heat to the surrounding medium. The action of these two forces on a system of particles may vary depending on the geometry of the system. Very notably, convective and thermophoretic effects are able to accumulate and trap colloids and macromolecules using the interplay between these two effects.¹⁵ Overall, thermal and convective forces (distinct from any optical interaction) in microfluidic systems offer a large degree of scope for manipulation that is only now being realized.

In this paper we demonstrate for the first time that controlled excitation of surface plasmon polaritons permits the use of combined optical and thermal forces for large-scale ordering of colloidal aggregations. We identify three regimes where different forces dictate the properties of the colloidal aggregation. The detailed behavior of the physical system is dictated by judicious choice of the sample chamber thickness and incident SPP excitation optical power. In the presence of excess thermal gradients, colloidal particles self-organize to create large extended two-dimensional colloidal hexagonal crystals. We ascribe this effect to dominance of convective forces drawing colloids to the center of the excited region. Under conditions where thermal gradients and hence convection are largely suppressed particles are accumulated at the center of the excited region and arranged into linear colloidal chains. In this case the observed colloid dynamics are asso-

ciated with a dominant optical interaction with a small thermal counterpart. By increasing the excitation power, an induced temperature gradient allows the emergence of thermophoretic forces, which balance the convective forces and causes accumulation, and trapping of colloids in an elliptical ring formation. This juxtaposition of forces provides a unique method for accumulating; ordering and segregating extended arrays of microscopic particles.

II. PARTICLE DYNAMICS UNDER SURFACE PLASMON EXCITATION

Experiments were performed on a Kretschmann prism-coupling geometry, permitting wide area illumination and full control of the incident angle. A sample chamber (1 cm diameter) containing aqueous, colloidal solutions was placed on top of the prism. The chamber depth was varied between $10\ \mu\text{m}$ and $100\ \mu\text{m}$. Solutions consisted of monodispersed $5\ \mu\text{m}$ silica ($n=1.4$ @ $589\ \text{nm}$) spheres in water. A $1064\ \text{nm}$ laser beam (10W, CW, Yb-fiber laser, IPG Corporation) was passed through a BK7 glass (right angle) prism resulting in an incident angle around 61.50° at the internal reflecting surface. In order to generate surface plasmon polaritons a thin ($40\ \text{nm}$) Au layer was thermally evaporated onto the bottom of the chamber. Excitation of the surface plasmons was achieved by tuning the incident angle around the resonant angle, which is just beyond the critical angle (total internal reflection). A minimum in reflectivity is observed with p -polarized light at the SPP resonance. Observations of the colloid dynamics in this system were performed with long working distance microscope objectives (Mitutoyo, $50\times$, $\text{NA}=0.42$ and $10\times$, $\text{NA}=0.28$), a CCD camera (PULNIX) and white light illumination.

Initial measurements were performed on $5\ \mu\text{m}$ silica spheres in a $100\ \mu\text{m}$ deep chamber. The obliquely incident Gaussian laser beam produced an elliptical spot at the sample surface. At an incident angle of 1.0° greater than the critical angle (62.5°), excitation of the SPP was observed. For an incident power of $600\ \text{mW}$ ($16\ \text{W}/\text{mm}^2$) we find a large-scale migration of microspheres radially towards the beam center and subsequent self-organization into an extended hexagonal close-packed array [Fig 1(top)]. Turning the laser off results in Brownian diffusion of the particle array, which could be rapidly reassembled by turning the laser on. Importantly, the particles do not adhere to the bottom surface but rather achieve equilibrium in their extended 2D array. This mechanism resulted in the rapid (several minutes) creation of hexagonal arrays containing in excess of 10 000 particles. Figure 1 (middle) is a Voronoi diagram showing the nearest neighbor packing arrangement for each colloid in the aggregation. In the plot each color-coded polygon is a Wigner-Seitz cell for a colloid with the number and dimensions of each side representing the position of adjacent colloids.¹⁶ From this plot we see that particles in the center of the formation show a predominantly hexagonal arrangement, while the outer periphery shows a more fluidlike state with no preferential arrangement. Figure 1(bottom) shows a graph of the mean particle velocity as a function of incident angle of the input laser and recorded reflectivity. We observe there is a

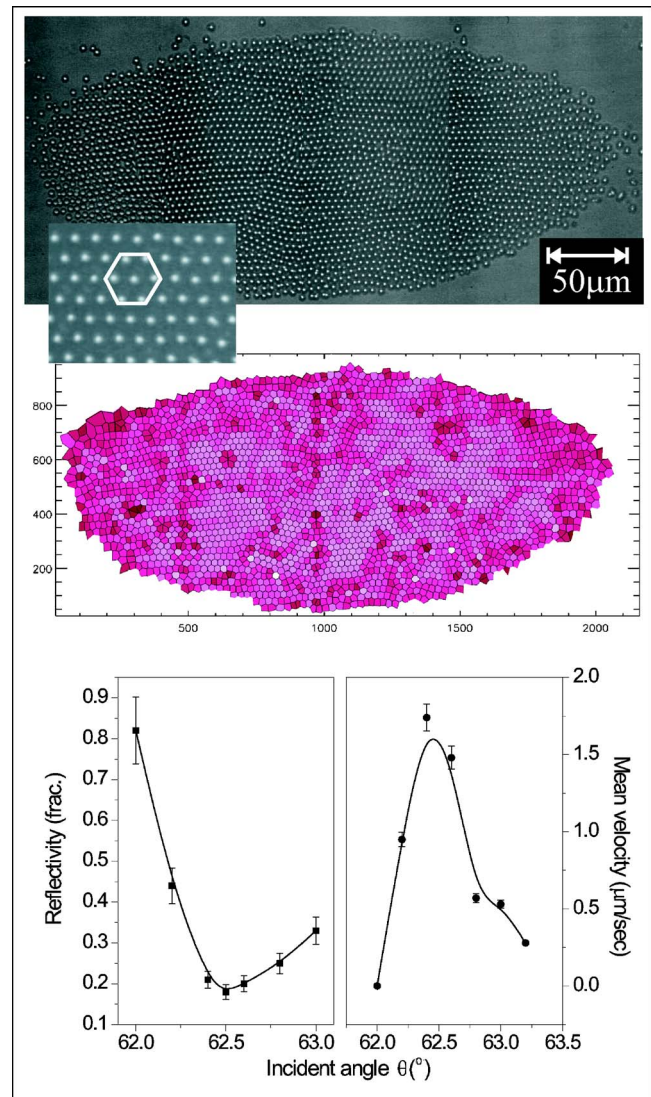


FIG. 1. (Color online) Top, SPP excitation in a 100 microns deep chamber results in crystal formation of a 2D hexagonal close packed structure. This figure shows an accumulated array of approximately 2800 particles. The image is a composite of 12 frames; inset shows hexagonal ordering. Middle, a Voronoi plot showing the Wigner-Seitz cell for each colloid in the aggregation indicates that at the center there is a predominantly closed-packed crystalline arrangement (hexagonal), where as at the periphery, particles are more fluidlike with no preferred nearest neighbor arrangement. Bottom, reflectivity of the incident light and mean velocity (curve is a guide to the eye) of the particles as a function of incident angle. Mean particle velocities were determined by tracking colloid motion over set interval ($100\ \mu\text{m}$) at a distance of $100\ \mu\text{m}$ from the center of the aggregation. Measurements were averaged over 20 particles for each incident angle.

direct correlation between the degree of excitation of the SPP (as recorded by the reflectivity) and the particle velocity. It is worth commenting further on the velocity observations: the minimum in reflectivity means the incident light energy is directly coupled to the SPP resonance. Notably, shifting only 1 degree from the SPP resonance condition is sufficient to ensure that the particle migration is halted offering a very

sensitive and effective method for migration control of such a large-scale colloidal aggregation.

The observed accumulation and ordering of colloids in the region of SPP excitation is fundamentally due to convection. As the SPP are confined to the Au layer, the dissipated heat transfer is localized at the bottom of the chamber and results in a thermal gradient along the depth of the chamber. When temperature gradients are present in the microfluidic chamber, convection acts to circulate fluid around the chamber in order to transfer heat to the colder regions. Thus fluid (and colloid) from adjacent cooler regions is drawn towards the center of the spot and then upward along the depth of the chamber. This is consistent with the observation of particles accumulating from regions beyond the directly illuminated spot. As gravity restricts the upward flow of the colloids, they aggregate about the center of the spot. By increasing the incident power, the gravitational forces may be overcome and the colloidal crystal is dispersed accompanied by strong convection-driven mixing. Ordering of colloids occurs naturally with increasing volume fraction and forms self-assembled hexagonally close-packed crystal arrays.¹⁷ These observations are in agreement with Duhr *et al.* who observed thermally driven colloidal crystallization by focusing a highly absorbing laser beam into the center of the sample chamber.¹⁸

Using the above chamber geometry, a mixture containing temperature dependent fluorescent dye (BCECF) and small colloids (0.5–1 μm) was used to simultaneously assess the extent of heating in the chamber under SPP excitation, and visualize the ensuing fluid dynamics. Temperature changes were monitored through intensity variations in the fluorescence spectrum of the BCECF dye, excited with the 490 nm line of a Hg lamp.¹⁹ The spectra were taken with a grating spectrometer (Jobin/Yvon TRIAX 550) and accompanying thermoelectrically cooled CCD camera. This was compared with calibration measurements from samples uniformly heated to known temperatures using an electrical heater. The temperature was monitored in the proximity of the gold surface using a thermocouple immersed in the chamber. The spectra obtained for three different temperature values are shown in Fig. 2(a). The observed decrease in intensity with increasing temperature is due to increased nonradiative losses resulting from molecular collisions. A plot of the peak of maximum intensity (538 nm wavelength) versus the temperature is shown in Fig. 2(b). It is observed that for mean temperature increases of up to 10 $^{\circ}\text{C}$ above room temperature, colloids are seen to aggregate in the center of the excited region, while laminar (i.e., nonturbulent and stable) convection rolls are clearly observed when the temperature is increased by 20 $^{\circ}\text{C}$. Although no temperature gradients were discerned in these measurements, there is a clear indication that excitation-dependent heating is present in the chamber and that changes in fluid dynamics are correlated with the temperature change.

Rusconi *et al.* shows that the convection velocity (U) in a thin chamber of thicknesses (l) containing lateral temperature gradient can be determined by balancing the buoyancy and kinematic viscosity forces and is given by

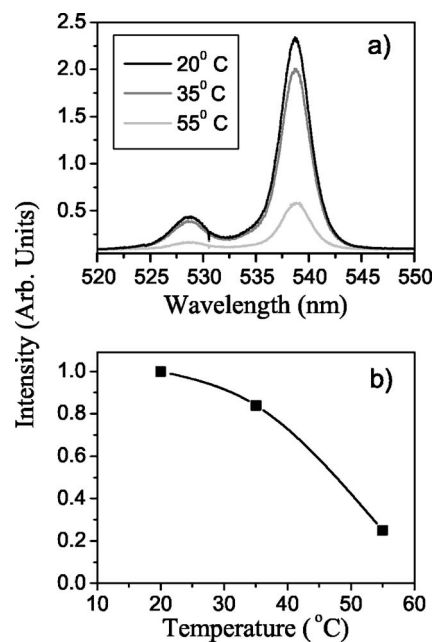


FIG. 2. A temperature dependent fluorescent dye (BCECF) was used to assess the extent of heating in the chamber under SPP excitation. (a) Shows fluorescence spectra from BCECF dye in the sample chamber when heated to a known temperature, measured using a thermocouple. The change in the peak intensity, (b), was used to estimate the sample temperature for different SPP excitation powers.

$$U \approx g\alpha_0 l^2 \Delta T / \nu,$$

where α_0 is the thermal expansion coefficient of the medium; ν is the kinematic viscosity; g is gravity; and ΔT is the vertical temperature gradient.²⁰ Simple calculations for the above-mentioned chamber geometry suggest that only a modest temperature gradient of 0.1 $^{\circ}\text{C}$ over the chamber depth (100 μm) is required to achieve the observed convection velocities.

III. OPTICALLY INDUCED ORDERING OF COLLOIDS

By reducing the chamber depth we suppress the vertical temperature gradient inside the sample solution, thereby diminishing the effect of convection. Subsequent experiments were performed on 5 μm silica spheres in a 10 μm deep chamber (depth 1/10 of the previous chamber). Using the new chamber geometry, radial accumulation is again observed at a slower rate at an excitation power of 160 mW (4.8 W/mm²). Figure 3 displays a still image of the typical arrangement of the colloids at the center of the excitation region. Remarkably, the accumulated colloids organize themselves into long (particle number $N > 20$) connected chains oriented in the direction of the SPP wave vector, and separated by regular intervals in the orthogonal direction. We can furthermore observe light scattering from one side of the spheres which is analogous to the behavior seen in standard evanescent wave guiding and trapping,⁹ showing that the optically enhanced SPP wave is now playing a role in particle aggregation.

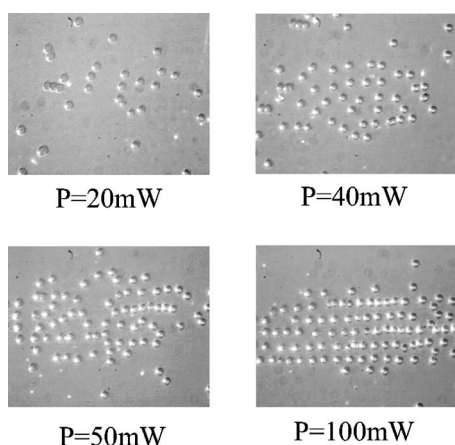


FIG. 3. Successive frames showing the behavior of colloidal particles ($5 \mu\text{m}$ diameter) as a function on increasing power in a thin sample chamber. We observe the formation of linear arrays as can be seen in frame 4 due to an enhanced optical interaction from the SPP excitation. Notably the power required to form such chains is approximately a factor of 3 less than that for standard evanescent wave with the same beam parameters.

The formation of colloidal chains has also been observed in other near field optical guiding experiments (e.g., Ref. 9). Here chains are formed when adjacent colloids are attracted via the optical gradient force to the asymmetric scattered light pattern produced by light coupled by the particles from the surface plasmon. The linear colloidal chains and inter-chain spacings are similar to optical binding phenomena described by Burns *et al.* and others,^{21,22} where perturbations of an optical field due to the presence of a microsphere influences the arrangement of surrounding microspheres. The scattered light pattern from individual colloids may also be observed in Fig. 3, and is seen to be strongly concentrated along the axis of the aligned colloids. The formation of this linear array of colloids is the first clear indication of a dominant optical interaction between colloids and surface plasmon excitation. Interestingly, the formation of chains is observed at powers lower than those observed in the case of pure evanescent wave excitation. Chain formation of colloids in standard evanescent wave trapping was observed with an input power of 300 mW (9.0 W/mm^2) as compared with 100 mW (3.0 W/mm^2) using surface plasmons in analogous situations. This difference is likely due to a modest enhancement of the electric field. Simple theoretical arguments suggest an increase in the amplitude of the evanescent field of greater than 20 times in the presence of surface plasmons.¹ The discrepancy between theoretical and experimental results may potentially be due to appreciable surface roughness in the thermally evaporated Au films. This significantly reduces the optical power coupled to surface plasmons and evidence of this is seen in the amount of reflected light (20%) observed on resonance (see Fig. 1). Reduced effects may also be due to residual thermal forces which act to deter long chain formation.

IV. EFFECT OF THERMOPHORESIS

By increasing the incident power we are able to increase the temperature gradients in the transverse direction and ob-

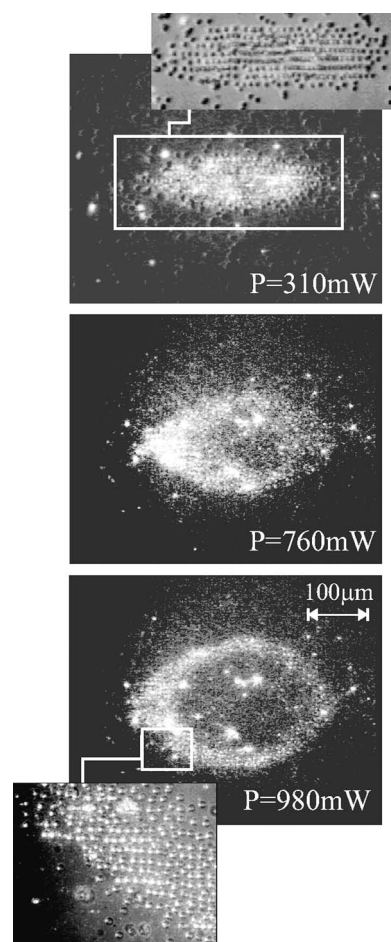


FIG. 4. Increasing the power in a thin chamber reveals lateral thermophoresis occurring which results in the repulsion of particles from the region of SPP excitation (hot to cold) and the arrangement of the repelled colloids into linear arrays in the periphery of the region. The frames show light scattered by the colloids (no white light illumination). The top and bottom inset are a detailed view (illuminated with white light) of the linear ordering of the accumulated particles.

serve the onset of thermophoretic forces. When this is done the colloids migrate away from the center of the excited region and form a distinct elliptical ring of colloids about the center of the spot. For increasing incident powers the area of the depleted region becomes greater, as is shown in Fig. 4. Notably, the colloids in the ring retain their linear array configuration indicating the continued dominance of the optical field. The presence of accumulation in a ring formation, which was first demonstrated by Braun *et al.* in DNA trapping studies,¹⁵ is evidence of the emergence of transverse thermophoretic forces, which balance the convective forces driving the colloids radially inward. For incident powers where thermophoresis exceeds convection at the center of the excited region, the colloids move radially outwards. The movement of colloids radially outwards (thermophoresis) is dependent on the transverse temperature gradient, whereas the inward flux of fluid and colloid (convection) is dependent on the temperature gradient in the normal direction. As the transverse temperature gradient reduces radially from the

center of the excited region, thermophoretic forces are diminished and an equilibrium position is reached at a radius where the two forces are balanced. As the normal temperature gradient is restricted by the small physical dimensions of the chamber ($10\ \mu\text{m}$), thermophoretic forces may be increased relative to convection and an equilibrium position may be obtained at arbitrary positions simply by controlling the incident power. More importantly, as thermophoretic forces arise from an interfacial interaction between the colloid and the surrounding fluid, microparticles of differing size and composition will have differing equilibrium positions. In turn this offers a new mechanism by which we may separate or fractionate micro-objects over large areas.

V. CONCLUSIONS

In conclusion we have successfully demonstrated the application of enhanced optical forces and optically induced thermal forces, generated by surface plasmon polariton excitation, for controlled aggregation, manipulation and ordering of large arrays of colloidal particles. We have identified a number of conditions where different competing forces dominate, leading to markedly different particle dynamics. Specifically, we have shown that under conditions where laminar convection may be freely established, particles are

observed to accumulate at the center of the excitation region and form hexagonal close-packed crystals. When convection forces are largely suppressed, in-plane thermal gradients act to move particle away from the excitation region (through thermophoresis) and resulting in the accumulation of particles in a ring formation. By minimizing all thermal effects colloids are observed to form regularly spaced arrays of linear chains, analogous to optically bound colloidal waveguides, under the influence of enhanced optical forces. Surface plasmon polariton excitation offers a powerful route for exploring the use of both thermal and enhanced optical forces for colloidal aggregation and in particular the interplay between these two differing but key forces in the microscopic regime.

ACKNOWLEDGMENTS

This work, as part of the European Science Foundation EUROCORES programme NOMSAN was supported by funds from the UK Engineering and Physical Sciences Research Council and the EC Sixth framework programme and the European Commission 6th framework programme—NEST ADVENTURE Activity—through Project ATOM-3D Contract No. 508952. The authors would like to thank G. Spalding for his contribution of the Voronoi plot.

*Author to whom correspondence should be addressed. Electronic address: kd1@st-and.ac.uk

- ¹H. Raether, *Surface Plasmons* (Springer-Verlag, Berlin, Heidelberg, 1988).
- ²W. L. Barnes, A. Dereux, and T. W. Ebbesen, *Nature (London)* **424**, 824 (2003).
- ³S. Sun and G. J. Leggett, *Nano Lett.* **4**, 1381 (2004).
- ⁴S. A. Maier, M. L. Brongersma, P. G. Kik, S. Meltzer, A. A. G. Requicha, and H. A. Atwater, *Adv. Mater. (Weinheim, Ger.)* **13**, 1501 (2001).
- ⁵K. Kneipp, H. Kneipp, I. Itzkan, R. R. Dasari, and M. S. Feld, *J. Phys. A* **14**, R597 (2002).
- ⁶N. Fang, H. Lee, C. Sun, and X. Zhang, *Science* **308**, 534 (2005).
- ⁷A. Ashkin, J. M. Dziedzic, J. E. Bjorkholm, and S. Chu, *Opt. Lett.* **11**, 288 (1986).
- ⁸H. Melville, G. F. Milne, G. C. Spalding, W. Sibbett, K. Dholakia, and D. McGloin, *Opt. Express* **11**, 3562 (2003).
- ⁹V. Garcés-Chávez, K. Dholakia, and G. C. Spalding, *Appl. Phys. Lett.* **86**, 031106 (2005).
- ¹⁰J. R. Arias-Gonzalez and M. Nieto-Vesperinas, *J. Opt. Soc. Am. A Opt. Image Sci. Vis* **20**, 1201 (2003).
- ¹¹T. Esslinger, M. Weidemüller, A. Hemmerich, and T. W. Hansch,

- Opt. Lett.* **18**, 450 (1993).
- ¹²H. B. Mao, J. R. Arias-Gonzalez, S. B. Smith, I. Tinoco, and C. Bustamante, *Biophys. J.* **89**, 1308 (2005).
- ¹³S. Masuo, H. Yoshikawa, H. G. Nothofer, A. C. Grimsdale, U. Scherf, K. Mullen, and H. Masuhara, *J. Phys. Chem. B* **109**, 6917 (2005).
- ¹⁴R. H. Farahi, A. Passian, T. L. Ferrell, and T. Thundat, *Opt. Lett.* **30**, 616 (2005).
- ¹⁵D. Braun and A. Libchaber, *Phys. Rev. Lett.* **89**, 188103 (2002).
- ¹⁶J. A. Weiss, D. W. Oxtoby, D. G. Grier, and C. A. Murray, *J. Chem. Phys.* **103**, 1180 (1995).
- ¹⁷Z. D. Cheng, W. B. Russell, and P. M. Chaikin, *Nature (London)* **401**, 893 (1999).
- ¹⁸S. Duhr and D. Braun, *Appl. Phys. Lett.* **86**, 131921 (2005).
- ¹⁹D. Braun and A. Libchaber, *Phys. Biol.* **1**, P1 (2004).
- ²⁰R. Rusconi, L. Isa, and R. Piazza, *J. Opt. Soc. Am. B* **21**, 605 (2004).
- ²¹M. M. Burns, J. M. Fournier, and J. A. Golovchenko, *Phys. Rev. Lett.* **63**, 1233 (1989).
- ²²S. A. Tatarkova, A. E. Carruthers, and K. Dholakia, *Phys. Rev. Lett.* **89**, 283901 (2002).